IAHR
AIRH

Journal of Hydraulic Research Vol. 46, No. 5 (2008), pp. 668–678
doi:10.3826/jhr.2008.2898

Application of Multi-Block method for simulating shallow free surface flows in complex geometries

Application de la méthode multi-blocs à la simulation des écoulements peu profonds à surface libre dans les géométries complexes

M.R. HADIAN, (IAHR Member), Assistant Professor, *Department of Civil Engineering, Faculty of Engineering, Yazd University, Pajouhesh St., Safaiyeh, Yazd, P. O. Box: 89195-741, Iran. Tel.: +98 351 8211671; fax: +98 351 8210699; e-mail: mr_hadian@yazduni.ac.ir*

A.R. ZARRATI, (IAHR Member), Associate Professor, *Department of Civil and Environmental Engineering, Amirkabir University of Technology, No. 424, Hafez Ave., 15914, Tehran, Iran. Tel.: +98 21 64543002; fax: +98 21 66414213; e-mail: zarrati@aut.ac.ir*

ABSTRACT
In the present study a numerical method is developed for simulating shallow free surface flows in complex geometries. A Multi-Block (MB) method is employed in conjunction with non-orthogonal curvilinear coordinate system. This technique gives the numerical method a high flexibility to tackle flow domains with any complex boundary which may be encountered in nature. The MB method utilizes patched grid with continuous grid lines across block boundaries. In this paper the MB methods is applied to 2-D shallow flows. However, this technique is extendable to 3-D models too. The model is based on collocated grid arrangement and the control volume method is used for solution of equations. The method is implicit and uses a SIMPLEC-like algorithm to find the water surface elevation. The flexibility and accuracy of the model is presented in few test cases with complex block arrangement and circulating flows.

RÉSUMÉ
Dans la présente étude une méthode numérique est développée pour simuler les écoulements peu profonds à surface libre dans les géométries complexes. On utilise conjointement une méthode multi-blocs et un système de coordonnées curvilignes non-orthogonales. Cela permet une grande souplesse pour traiter les domaines d'écoulement quelle que soit la complexité des frontières rencontrées en nature. La méthode multi-blocs utilise un maillage rapiécé avec des lignes de maillage continues à travers les frontières de bloc. Dans cet article la méthode multi-blocs est appliquée aux écoulements 2-D peu profonds. Mais cette technique est également applicable aux modèles 3-D. Le modèle est basé sur une disposition de grille colocalisée et on utilise la méthode du volume de contrôle pour la solution des équations. La méthode est implicite avec un algorithme de type SIMPLEC pour déterminer l'élévation de la surface libre. La souplesse et l'exactitude du modèle sont illustrées par quelques cas tests présentant une certaine complexité dans la disposition des blocs et la circulation des écoulements.

Keywords: Complex geometry, depth correction, free surface, implicit, multi block, numerical model, shallow-flow

1 Introduction

During the past decade the extraordinary development in computer power for processing and available memory for storing a large number of data and variables has led to increasingly use of CFD in fluid-flow problems. Flow in nature is three dimensional (3-D). However, in many cases of river and coastal engineering the vertical acceleration of water is negligible compared to the gravitational acceleration. In these conditions the equations of motion can be integrated in depth to derive two dimensional depth averaged equations. Although this model may not be very accurate in regions with sharp gradients of water surface profile and strong secondary flows, but it is accurate enough for many practical purposes. Numerical solution of 2D shallow water equations has been performed for more than 30 years from the early works of Kuipers and Vreugdenhil (1973). Since then several other research works have also been published such as studies by: McGuirk and Rodi (1978), Vregdenhill and Wijbenga (1982), Chapman and Kuo (1985), Tingsanchali and Maheswaran (1990), Molls and Chaudhry (1995), Ye and McCorquodale (1997), Klonidis and Soulis (2001) and Weerakoon *et al.* (2003).

One of the problems in CFD is the complexity of flow domains. To solve this problem different strategies and schemes are used by researchers. Using unstructured mesh is one of the methods developed to deal with complexities of the flow domain. The main weak point of unstructured grids is the more computer memory that is needed to store some matrices which define the nodes of each cell and connectivity between cells. Working with such matrices

Revision received April 26, 2007/Open for discussion until April 30, 2009.

needs more attention in computer programming and increases the required CPU time which is not desirable. Another method in dealing with complex boundaries is utilizing curvilinear coordinates. The curvilinear coordinate system has the limitation for generating appropriate mesh in very complex flow domains. For instance, cases with sharp changes in flow boundaries leads to a very poor numerical mesh, considering the smoothness and mesh skewness. This results in inaccuracy and problems in convergence for some of CFD techniques (Wijbenga,1985; Peric,1990). A general method to deal with this problem in complex flow domains is the Multi-Block (MB) technique. In this technique the flow domain is decomposed to some sub-domains (blocks) and the equations are solved in every block separately. In the present work the MB method is used in conjunction with curvilinear coordinate system to tackle with any complex boundary which may be encountered in nature. This includes sharp and curved boundaries, channel bifurcation or confluence and existence of obstacles in the flow domain such as bridge piers.

1.1 The Multi-Block method

The MB method has been studied and widely used in CFD problems (Shyy *et al.*, 1997; Sinha *et al.*, 1998; Apsley and Hu, 2003; Zhang et al., 2004). Decomposing the flow domain can be done by using one of the two MB configurations, i.e. patched or overlapping grids (Fig. 1). In both patched and overlapping grids, transferring data between neighboring blocks is the most important issue which needs special attention. In patched grid with non-common nodes on block boundaries interpolation is needed for passing data between neighboring blocks, also the conservation of fluxes across the boundaries needs special attentions. In overlapping blocks the transformation of data between neighboring blocks is more complex and needs interpolation. For interpolation, accuracy and conservation are two issues which affect the results of different methods and should be compromised. Usually interpolations with higher orders of accuracy do not satisfy the conservation of fluxes and conservative methods of interpolation are not so accurate. Shyy *et al.* (1994) stated that "simultaneous achievement of both conservation and accuracy is very difficult in some cases". Among many studies for solving this problem Henshaw (1994), Hinatsu and Ferziger (1991), and Meakin and Street (1988) applied direct interpolation of variables across the blocks, while Zhang *et al.* (2004), Shyy *et al.* (1994), Tu and Fuch (1992), and Wright and Shyy (1993) used a conservative scheme to achieve an accurate interpolation.

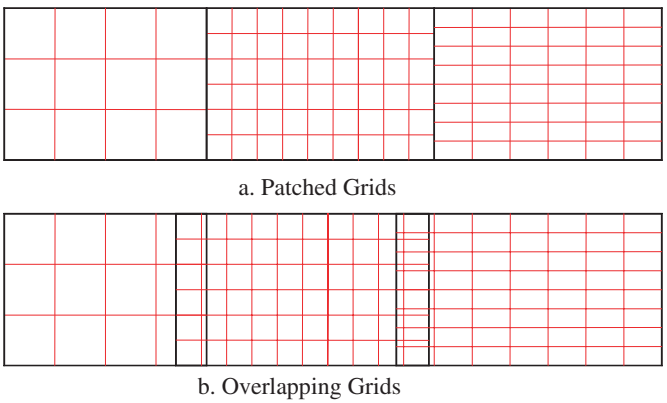

a. Patched Grids

b. Overlapping Grids

Figure 1 Schematic explanation of patched grid blocks and overlapping blocks

To avoid the difficulty of losing accuracy or conservation in overlapping grids and to reduce the CPU time by reducing interpolations and complex data structures, the method of Lien *et al.* (1996) is developed in the present study to tackle shallow water equations. Shallow water equations consist of water depth and in addition to velocities, depths also change in the process of numerical solution, which this may endanger the convergence.

The main objective of the present study is to show the flexibility of MB method in solving shallow water equations. Using this technique the flow with complex boundaries could be simulated in a very straightforward manner. The robustness of the model is presented by simulating the flow profile in a straight channel divided into several blocks, flow at side intake and jet forced flow passing a circular basin. The numerical results are compared with available experimental data and other published numerical results.

2 Governing equations

Neglecting wind shear stress, Coriolis acceleration, and using Boussinesq approximation for Reynolds stresses, the conservative form of 2-D shallow water equations can be written in general curvilinear coordinate system in the following form. Partial transformation is used here with Cartesian velocities as primary variables, which read:

$$\frac{\partial \zeta}{\partial t} + \frac{1}{J}\left(\frac{\partial}{\partial \xi}(Uh) + \frac{\partial}{\partial \eta}(Vh)\right) = 0 \tag{1}$$

$$\begin{aligned} &J\frac{\partial}{\partial t}(hu) + \frac{\partial}{\partial \xi}(hUu) + \frac{\partial}{\partial \eta}(hVu) \\ &\quad - \frac{\partial}{\partial \xi}\left[\frac{\nu_e}{J}\left(q_{11}\frac{\partial hu}{\partial \xi} - q_{12}\frac{\partial hu}{\partial \eta}\right)\right] \\ &\quad + \frac{\partial}{\partial \eta}\left[\frac{\nu_e}{J}\left(q_{22}\frac{\partial hu}{\partial \eta} - q_{12}\frac{\partial hu}{\partial \xi}\right)\right] = S_u \end{aligned} \tag{2}$$

$$\begin{aligned} &J\frac{\partial}{\partial t}(hv) + \frac{\partial}{\partial \xi}(hUv) + \frac{\partial}{\partial \eta}(hVv) \\ &\quad - \frac{\partial}{\partial \xi}\left[\frac{\nu_e}{J}\left(q_{11}\frac{\partial hv}{\partial \xi} - q_{12}\frac{\partial hv}{\partial \eta}\right)\right] \\ &\quad + \frac{\partial}{\partial \eta}\left[\frac{\nu_e}{J}\left(q_{22}\frac{\partial hv}{\partial \eta} - q_{12}\frac{\partial hv}{\partial \xi}\right)\right] = S_v \end{aligned} \tag{3}$$

In which, u and v are depth averaged Cartesian velocities, U and V are depth averaged contravariant velocity components in general curvilinear ξ and η directions respectively, h is the water depth, ρ is the water density, ν_e is the depth averaged effective viscosity ($\nu_e = \nu + \nu_t$), ν is the kinematic viscosity of fluid, ν_t is the depth averaged turbulent viscosity, g is the gravitational

acceleration, ζ is the water surface elevation ($\zeta = h + Z_b$), Z_b is the bed elevation, J is the jacobian of transformation ($J = x_\xi y_\eta - x_\eta y_\xi$) where x_ξ, x_η, y_ξ and y_η are metrics, τ_{bx} and τ_{by} are bed shear stresses in x and y directions. These stresses can be calculated from Manning's equation as:

$$\frac{\tau_{bx}}{\rho} = \frac{g\,n^2\,u\sqrt{u^2+v^2}}{h^{1/3}}, \quad \frac{\tau_{by}}{\rho} = \frac{g\,n^2\,v\sqrt{u^2+v^2}}{h^{1/3}} \tag{4}$$

Other parameters are defined as below:

$$\begin{aligned} S_u = {} & \frac{\partial}{\partial\xi}\left[\frac{\nu_e}{J}\left(y_\eta\frac{\partial Uh}{\partial\xi} - y_\xi\frac{\partial Uh}{\partial\eta}\right)\right] \\ & + \frac{\partial}{\partial\eta}\left[\frac{\nu_e}{J}\left(y_\eta\frac{\partial Vh}{\partial\xi} - y_\xi\frac{\partial Vh}{\partial\eta}\right)\right] \\ & - gh\left(y_\eta\frac{\partial\zeta}{\partial\xi} - y_\xi\frac{\partial\zeta}{\partial\eta}\right) - J\frac{\tau_{bx}}{\rho} \end{aligned} \tag{5}$$

$$\begin{aligned} S_v = {} & \frac{\partial}{\partial\xi}\left[\frac{\nu_e}{J}\left(-x_\eta\frac{\partial Uh}{\partial\xi} + x_\xi\frac{\partial Uh}{\partial\eta}\right)\right] \\ & + \frac{\partial}{\partial\eta}\left[\frac{\nu_e}{J}\left(-x_\eta\frac{\partial Vh}{\partial\xi} + x_\xi\frac{\partial Vh}{\partial\eta}\right)\right] \\ & - gh\left(x_\xi\frac{\partial\zeta}{\partial\eta} - x_\eta\frac{\partial\zeta}{\partial\xi}\right) - J\frac{\tau_{by}}{\rho} \end{aligned} \tag{6}$$

$$q_{11} = x_\eta^2 + y_\eta^2, \quad q_{12} = x_\xi x_\eta + y_\xi y_\eta, \quad q_{22} = x_\xi^2 + y_\xi^2 \tag{7}$$

The depth averaged contravariant velocity components, which are tangential to curvilinear coordinate ξ and η respectively, are defined as:

$$U = uy_\eta - vx_\eta, \quad V = vx_\xi - uy_\xi \tag{8}$$

The depth averaged turbulent viscosity is calculated by the following equation:

$$\nu_t = \frac{\kappa}{6}u_* h \tag{9}$$

In which u_* is the bed shear velocity and κ is the von Karman constant ($= 0.4$).

3 Numerical scheme and solution algorithm

For the numerical solution of the governing equations, mesh should be generated and overlaid on the flow domain. Variables could be stored at cell centers and cell faces. To avoid the checker board water depth oscillation one can use the staggered grid arrangement or use collocated grid in conjunction with momentum interpolation for cell face velocities. However, implementation of the MB method is much easier with collocated grid than staggered grid. In addition, in collocated grids only one kind of control volume is assumed which makes it more straightforward for programming and implementation of boundary conditions. Therefore, the collocated grid arrangement is used in the present study with momentum interpolation for calculating cell face velocities (Fig. 2).

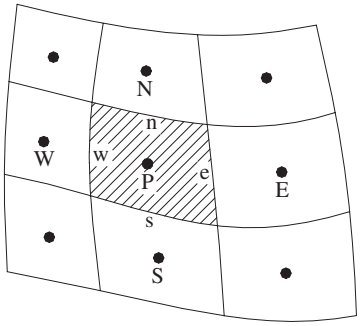

Figure 2 Control volumes in a collocated grid arrangement

3.1 Discretization of the governing equations

Based on control volume method the momentum equations in x and y directions can be discretized by integrating the equations through control volume and time (Patankar, 1980).

Usually the second order central difference is used for diffusion terms; however the convection terms need special attention. The first order upwind scheme is one of the most stable schemes and is used in many codes, but it suffers from numerical diffusion which affects the accuracy of the model. Here the UMIST-TVD scheme is used for convection terms (Lien and Leschziner, 1994a).

For time integration the first order Euler scheme and second order Crank–Nicolson scheme are the more popular ones in CFD. Since in the present work steady flows are studied, the first order full implicit Euler scheme has the required accuracy and is therefore employed.

All governing equations can be expressed in the following general form:

$$\begin{aligned} & J\frac{\partial}{\partial \mathrm{t}}(h\phi) + \frac{\partial}{\partial\xi}(Uh\phi) + \frac{\partial}{\partial\eta}(Vh\phi) \\ & - \left\{\frac{\partial}{\partial\xi}\left(\Gamma_\phi\frac{q_{11}}{J}\frac{\partial(h\phi)}{\partial\xi}\right) + \frac{\partial}{\partial\eta}\left(\Gamma_\phi\frac{q_{22}}{J}\frac{\partial(h\phi)}{\partial\eta}\right)\right\} = S_\phi \end{aligned} \tag{10}$$

which Γ_ϕ stands for diffusion coefficient of the variable ϕ. Note that the cross diffusive terms are transferred to source term. Also the linearization of source term is used which absorbs the bed shear stress of momentum equations. It can be shown that under relaxation factors are useful in reducing the computational time (see Sec. 5). Following the notation of Patankar (1980), discretized equations after the effect of under-relaxation factor are expressed as:

$$\frac{A_p}{\alpha_\phi}\phi_p = \sum_{\mathrm{nb=E,W,N,S}} A_{\mathrm{nb}}\phi_{\mathrm{nb}} + \frac{1-\alpha_\phi}{\alpha_\phi}A_p\phi_p^{**} + A_p^{\mathrm{o}}\phi_p^{\mathrm{o}} + S_\phi \tag{11}$$

In this equation the "**" and "o" superscript denoted the values of previous iteration and previous time step, respectively. The coefficients for first order upwind scheme are as:

$$\begin{aligned} A_E &= D_e + \max(-F_e, 0) \quad A_W = D_w + \max(F_w, 0) \\ A_N &= D_n + \max(-F_n, 0) \quad A_S = D_s + \max(F_s, 0) \end{aligned} \tag{12}$$

$$A_p^{\circ} = (Jh^{\circ})_p \frac{\Delta\xi\Delta\eta}{\Delta t} \tag{13}$$

$$A_p = \sum_{\mathrm{nb}=E,W,N,S} A_{\mathrm{nb}} - S_p + (J\,h)_p \frac{\Delta\xi\,\Delta\eta}{\Delta t} \tag{14}$$

while F_i and D_i are convective and diffusive fluxes and defined as:

$$\begin{aligned} F_e &= (hU)_e \Delta\eta \quad F_w = (hU)_w \Delta\eta \\ F_n &= (hV)_n \Delta\xi \quad F_s = (hV)_s \Delta\xi \end{aligned} \tag{15}$$

$$\begin{aligned} D_e &= \left(\frac{\Gamma_\phi q_{11} h}{J\Delta\xi}\right)_e \Delta\eta \quad D_w = \left(\frac{\Gamma_\phi q_{11} h}{J\Delta\xi}\right)_w \Delta\eta \\ D_n &= \left(\frac{\Gamma_\phi q_{22} h}{J\Delta\eta}\right)_n \Delta\xi \quad D_s = \left(\frac{\Gamma_\phi q_{22} h}{J\Delta\eta}\right)_s \Delta\xi \end{aligned} \tag{16}$$

To avoid numerical diffusion of first order upwind scheme and preventing oscillation and over/under shooting of high order schemes the UMIST-TVD scheme of Lien and Leschziner (1994a) is used which employs the TVD filter in conjunction with QUICK scheme. To implement this high order discretization method, the negative coefficients in discretized governing equations (11) is prevented by means of *deferred correction* method. In which the coefficients are calculated by a stable first order upwind scheme and extra terms are added to the source term and are calculated explicitly (Ferziger and Peric, 1996). The required source term for UMIST-TVD scheme which should be added to source term of equations is (Lien and Leschziner, 1994a):

$$S_\phi^{\text{UMIST-TVD}} = 0.5 \left\{ \begin{aligned} &[F_e^+\varphi(r_e^+) - F_e^-\varphi(r_e^-)](\phi_E - \phi_P) \\ &-[F_w^+\varphi(r_w^+) - F_w^-\varphi(r_w^-)](\phi_P - \phi_W) \\ &+[F_n^+\varphi(r_n^+) - F_n^-\varphi(r_n^-)](\phi_N - \phi_P) \\ &-[F_s^+\varphi(r_s^+) - F_s^-\varphi(r_s^-)](\phi_P - \phi_S) \end{aligned} \right\} \tag{17}$$

In which:

$$\varphi(r) = \max(0, \min(2r, 0.25 + 0.75r, 0.75 + 0.25r, 2)) \tag{18}$$

$$F_i^{\pm} = 0.5(F_i \pm |F_i|) \tag{19}$$

$$\begin{aligned} r_e^+ &= \frac{\phi_P - \phi_W}{\phi_E - \phi_P} \qquad r_e^- = \frac{\phi_E - \phi_{\mathrm{EE}}}{\phi_P - \phi_W} \\ r_w^+ &= \frac{\phi_W - \phi_{\mathrm{WW}}}{\phi_P - \phi_W} \quad r_w^- = \frac{\phi_P - \phi_E}{\phi_W - \phi_P} \end{aligned} \tag{20}$$

3.2 Velocity-water surface elevation coupling

Water surface elevation appears in the continuity equation and in fact in explicit methods could be directly calculated from this equation. However in an implicit scheme, if the continuity equation is discretized to an algebraic equation for flow depth, some of the coefficients may become negative. This is in contrast with the second rule presented by Patankar (1980) for obtaining results which ensure physical realism and overall balance. Here a SIMPLEC-like algorithm is used for coupling between water surface elevation and velocities.

If values of contravariant velocity components achieved from momentum equation and the water surface elevation related to last iteration are shown by an asterisk sign, one can write:

$$U + U^* + U', \quad V = V^* + V', \quad \zeta = \zeta^* + \zeta'(h = h^* + h') \tag{21}$$

Where prime shows the correction required for obtaining the values which satisfy the continuity equation. In the SIMPLEC algorithm the contravariant velocity corrections are:

$$U' = -B\frac{\partial\zeta'}{\partial\xi}, \quad B = \frac{g\,h\,q_{11}\Delta\xi\,\Delta\eta}{\dfrac{A_p}{\alpha_{u,v}} - \sum A_{\mathrm{nb}}} \tag{22}$$

$$V' = -C\frac{\partial\zeta'}{\partial\eta}, \quad C = \frac{g\,h\,q_{22}\Delta\xi\,\Delta\eta}{\dfrac{A_p}{\alpha_{u,v}} - \sum A_{\mathrm{nb}}} \tag{23}$$

Applying Eqs. (21)–(23) in the continuity equation results in the following equation for correction of water surface elevation:

$$\begin{aligned} &J\frac{\partial\zeta'}{\partial t} + \frac{\partial}{\partial\xi}(U^*\zeta') + \frac{\partial}{\partial\eta}(V^*\zeta') - \frac{\partial}{\partial\xi}\left(Bh^*\frac{\partial\zeta'}{\partial\xi}\right) - \frac{\partial}{\partial\eta}\left(Ch^*\frac{\partial\zeta'}{\partial\eta}\right) \\ &\quad = -\left[J\frac{\partial\zeta^*}{\partial t} + \frac{\partial}{\partial\xi}(U^*h^*) + \frac{\partial}{\partial\eta}(V^*h^*)\right] \end{aligned} \tag{24}$$

The above equation is a convection-diffusion equation which can be discretized using any appropriate method. In the present work central difference scheme is used for both convention and diffusion terms. The right hand side of the equation is the residual of mass that will be zero when the solution converges. Therefore the sum of the absolute value of the right hand side of Eq. (24) is considered as one of the criteria of convergence.

3.3 Momentum interpolation

To avoid the checker board water surface fluctuation in collocated grid arrangement the momentum interpolation method is used. Various methods have been developed for momentum interpolation, however results of these methods are dependent on under relaxation factors and the time step (Rhie and Chow, 1983; Majumdar, 1988; Miller and Schmidt, 1988; Wang and Komori, 1999; Choi, 1999; Olsen, 2000; Yu *et al.*, 2002a).

Yu *et al.* (2002b) presented two methods which were suitable for equations in Cartesian coordinate system and needed storing and interpolating terms involved in A_p. Another momentum interpolation method was presented by Lien and Leschziner (1994b). In their method all of the terms including the cell center velocities at previous time step, previous iterate and present iterate and pressure gradients are involved in the interpolation. In this method all of the Cartesian velocity components at previous time step and iteration are needed on every face and should be stored.

In the present study the method of Lien and Leschziner (1994b) is developed for shallow water equations. Considering Eqs. (15) and (24), only the contravariant valocities are required on cell faces (U on east and west faces and V on north and south faces). Therefore, the equations for cell face Cartesian velocities

components are combined and one contravariant velocity component is calculated for each face. This can considerably reduce the required computer memory and calculations. Using weighted interpolations by f_1 and f_2 factors in ξ and η directions respectively, the cell face contravariant velocity components on east and north faces are:

$$U_e = \left\{ \begin{array}{l} f_1 \left\{ A_P[U_P - (1-\alpha_v)\, U_P^{**}] - \alpha_v\, A_P^{o} U_P^{o} \\ + \alpha_v\, (g\, h\, q_{11}\, \Delta\xi\, \Delta\eta)_P \left(\dfrac{\partial \zeta}{\partial \xi}\right)_P \right\} \\ + (1-f_1) \left\{ A_E \left[U_E - (1-\alpha_v)\, U_E^{**}\right] \right. \\ \left. - \alpha_v\, A_E^{o} U_E^{o} + \alpha_v\, (g\, h\, q_{11}\, \Delta\xi\, \Delta\eta)_E \left(\dfrac{\partial \zeta}{\partial \xi}\right)_E \right\} \end{array} \right\} \frac{1}{A_e} + (1-\alpha_v) U_e^{**} + \left\{ \alpha_v\, A_e^{o} U_e^{o} - \alpha_v\, (g\, h\, q_{11}\, \Delta\xi\, \Delta\eta)_e \left(\frac{\partial \zeta}{\partial \xi}\right)_e \right\} \frac{1}{A_e} \tag{25}$$

$$V_n = \left\{ \begin{array}{l} f_2 \left\{ A_P[V_P - (1-\alpha_v) V_P^{**}] - \alpha_v\, A_P^{o} V_P^{o} \\ + \alpha_v (g\, h\, q_{22}\, \Delta\xi\, \Delta\eta)_P \left(\dfrac{\partial \zeta}{\partial \eta}\right)_P \right\} \\ + (1-f_2) \left\{ A_N[V_N - (1-\alpha_v) V_N^{**}] \right. \\ \left. - \alpha_v\, A_N^{o} V_N^{o} + \alpha_v (g\, h\, q_{22}\, \Delta\xi\, \Delta\eta)_N \left(\dfrac{\partial \zeta}{\partial \eta}\right)_N \right\} \end{array} \right\} \frac{1}{A_n} + (1-\alpha_v) V_n^{**} + \left\{ \alpha_v\, A_n^{o} V_n^{o} - \alpha_v\, (g\, h\, q_{22}\, \Delta\xi\, \Delta\eta)_n \left(\frac{\partial \zeta}{\partial \eta}\right)_n \right\} \frac{1}{A_n} \tag{26}$$

In which α_v is the under-relaxation factor for momentum equations.

3.4 Boundary conditions and initial values

Based on the characteristic method, the number of boundary conditions in a flow domain is equal to the number of characteristic lines, which comes into the flow domain from the boundaries. For sub-critical flow regime, zero depth gradient is considered at inlet. Since discharge is known, inlet velocity is calculated by dividing the discharge by inlet cross sectional area.

At the outlet, water depth is fixed and velocity is assumed normal to the outlet section. No-slip boundary condition is considered for the solid walls, which implies using wall function presented by Launder and Spalding (1974).

At the beginning of the computation, the flow depth and flow velocities should be given to the model as the initial condition. In the present study the water depth at the outlet is assumed as flow depth in the entire flow domain and velocities at all the points are calculated using the flow discharge and assumed water depth.

The implementation of boundary conditions in MB technique is presented in details in the following section.

4 Implementation of the Multi-Block method

To use the MB method in the present study, the flow domain is divided into an arbitrary number of non-overlapping sub-domains or blocks in an unstructured topology based on the method of Lien *et al.* (1996). A structured non-orthogonal grid is generated in each block assuming the continuity of grid line positions across the block boundaries. This method makes the model very flexible to be used in any complex geometry.

To facilitate transformation of data across the blocks, a halo region with two layers of cells is assumed around each block (Fig. 3). In another word, each block is assumed to penetrate into its neighboring blocks with extent of two cell layer. All data belonging to these halo cells are stored in the data structure of

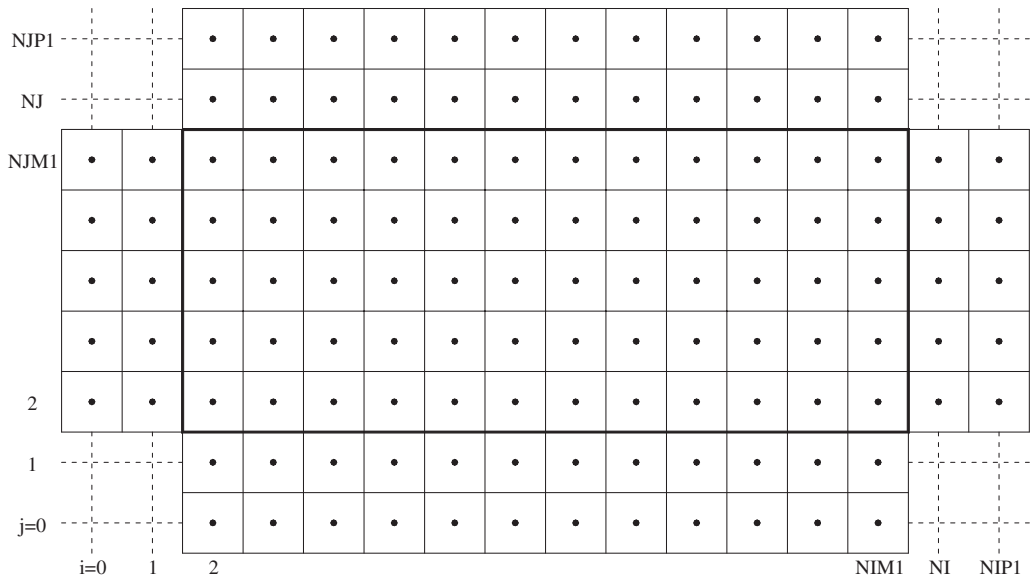

Figure 3 Halo cells around a block and its notation

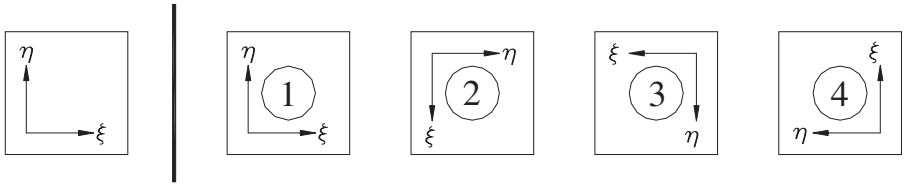

Figure 4 Assumed possible local coordinate system in blocks adjacent to any reference block

the parent block. Some of these data are fixed during the calculations, e.g. metrics and some of variables should be updated during calculations, e.g. velocities and water depths. The number of cell layers across the halo region depends on the order of accuracy used in the numerical methods. For the methods used in this study the stencil of discretization needs two layer of cells around each cell.

Since the blocks are assembled as unstructured block arrangement, two matrixes are required to store the connectivity between blocks and coordinate direction of neighboring blocks. Here similar to Lien *et al.* (1996) neighboring blocks are specified by their numbers. In addition 0, −1, −2 and −3 are used for solid wall, inlet, outlet and symmetric boundaries respectively.

To distinguish the direction of local coordinate in each neighboring block, Lien *et al.* (1996) considered all possible types of coordinate directions (8 types). However, four types of these coordinate directions are not right handed and result in negative value for jacobian which is not desirable. Therefore, only four types of coordinate directions were considered here introduced by codes 1 to 4 as shown in Fig. 4 and 0 is used for physical boundaries (i.e. walls, inlets and outlets). The codes of coordinate system of the neighbors of each block are stored in a matrix and are necessary for transferring the data across neighboring blocks. As an example, the connectivity matrix and coordinate direction matrix for an arbitrary domain decomposed into 3 blocks are shown in Fig. 5.

Using the two mentioned matrixes the transformation of data between neighboring blocks can be handled easily. Special attention should be paid for transformation of contravariant velocities or any grid oriented values, since they are dependent on curvilinear coordinate directions which can be different for a cell while

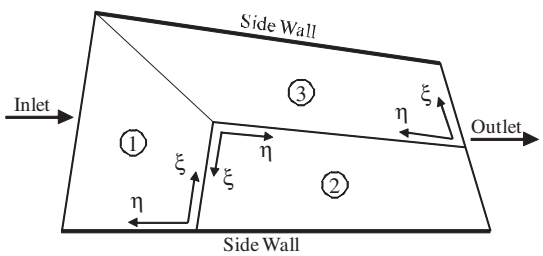

Connectivity Matrix

Block	east	west	north	south
1	3	0	-1	2
2	0	3	-2	1
3	0	2	1	-2

Coordinate Matrix

Block	east	west	north	south
1	4	0	0	3
2	0	3	0	3
3	0	3	2	0

Figure 5 Connectivity and coordinate matrixes for an arbitrary domain and assumed blocks

it is in its own block or when it is assumed as a halo cell of its neighboring block.

At physical boundaries the halo cells can be used for easier implementation of boundary conditions. At solid walls, negative value of the contravariant velocity at the nearest cell to the wall can be set at the halo cell in a way that the velocity perpendicular to the wall becomes zero. Moreover wall shear stress should be calculated by wall function and its components in x and y directions must be added to momentum equations.

At the outlet section (in sub-critical flow regime) the downstream water surface elevation are introduced to the model and these values are given to the halo cells of these boundaries. At inlet section, the contravariant velocity component parallel to flow direction and water surface elevation at halo cells are calculated assuming zero gradient condition from adjacent cells of the flow domain. Velocities are then needed to be corrected considering the flow discharge.

The procedure of solution at every time step can be summarized as follows:

- Solve the momentum equations for all block assuming fixed velocities at halo cells (frozen halo cells) in each block and then update the velocities in the entire flow domain including in halo cells.
- Solve the depth correction Eq. (24) for all blocks using frozen halo cells and then update ζ' in halo cells.
- Correct the water surface elevation, water depth and all velocities at all blocks (Eq. (21)) and update the halo cells.
- Considering the inlet discharge correct the velocities at inlet sections.
- Solve the equations for other scalar parameters, calculate turbulent eddy viscosity and update the halo cells.
- Repeat the above steps till convergence is achieved.
- Go to the next time step.

5 Model verification

In the first test case, a horizontal channel was assumed 40 m long and 2 m wide. Flow discharge was 1 m^3/s and Manning's roughness coefficient was assumed equal to 0.03. Tail water was fixed at 0.3 m at downstream of the channel. This depth is very close to critical depth and therefore the formed H2 profile has a sharp water surface gradient close to the outlet section. Water surface profile as calculated by the model is compared with the direct step method (Chow, 1959) in Fig. 6. Results show a good agreement between the present model and Direct Step Method.

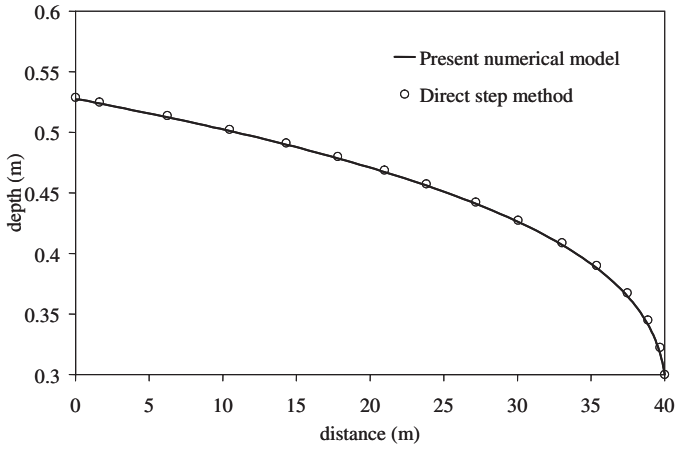

Figure 6 H2 profile along a channel

This example was then simulated using 8 different block configurations as shown in Fig. 7. The result of the model for all these configurations was exactly the same. It should be noticed that the CPU time increased as the number of blocks increased. So it is recommended not to decompose the flow domain to an unnecessary large number of blocks (Lai *et al.*, 1996). Figure 7 shows the coordinate of the blocks in different directions is different block configurations. Selecting coordinates in different directions was performed to assure that transferring of data between the blocks is correctly done. Another complexity that occurs in Test4 to Test8 (Fig. 7) of this example is the presence of more than one block at the inlet section. The computer code could distinguish all blocks located at each inlet sections and calculate the inflow discharge. This calculated discharge is then compared with the given discharge of the inlet at each time step and the velocities will be corrected accordingly. For example, in Test5 the inlet discharge is the sum of fluxes passing the south side of block 1(considering its local coordinate system) and east side of block 2. For block 1, $\sum Vh\Delta\xi$ should be calculated at the south side and be added to $\sum Uh\Delta\xi$ at the east side of block 2. Velocities at inlet sections should then be corrected considering the given discharge of this inlet section. The model is therefore applicable for more than one inlet section with complex system of blocks and different coordinate directions.

The second test case is the flow condition at a side intake perpendicular to main channel as is shown in Fig. 8 based on the experiment of Shettar and Murthy(1996). This case has one inlet section and 2 outlet section. Both the main channel and side intake are 0.3 m width. Manning roughness coefficient is set to 0.011 and the inlet discharge is 5.67 l/s. Tail water elevations at the outlet section of main and side channel are 0.055 m and 0.045 m respectively. The flow domain was divided into 4 blocks (Fig. 8) using $94 * 22$ cells at main channel and $36 * 22$ cells at side channel. The generated grid is non-uniform in both

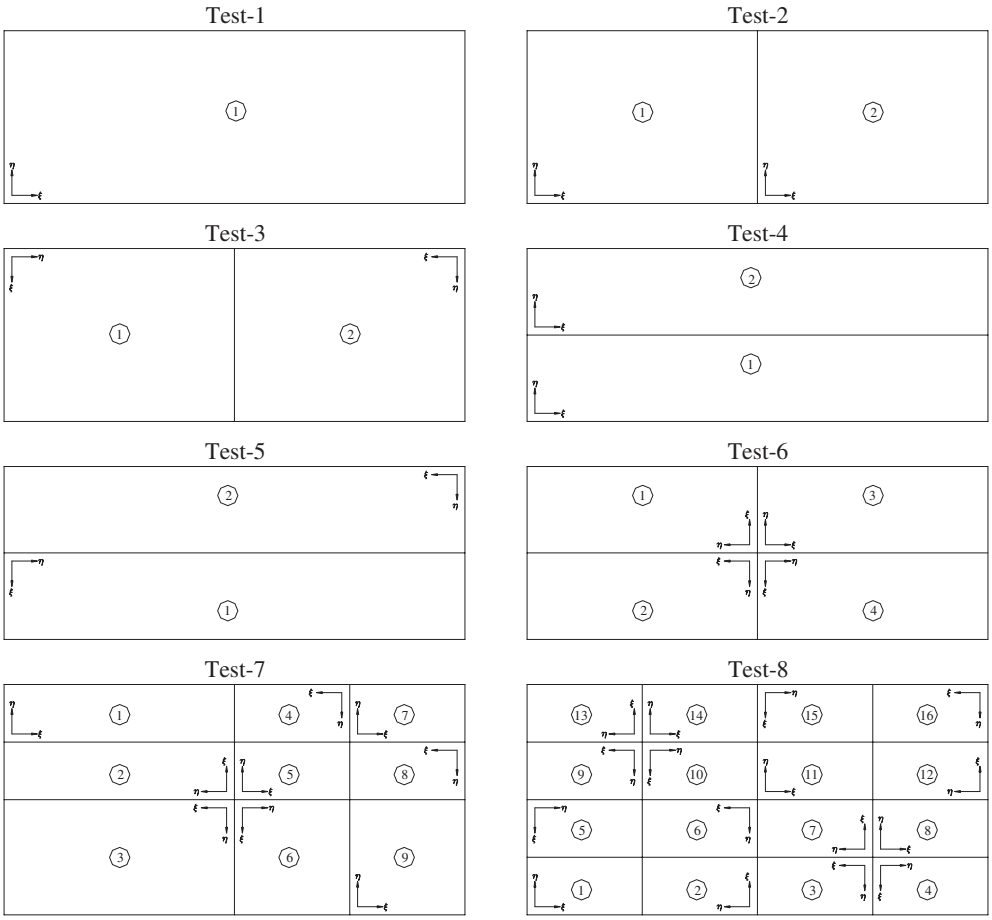

Figure 7 Different block topologies for the rectangular channel

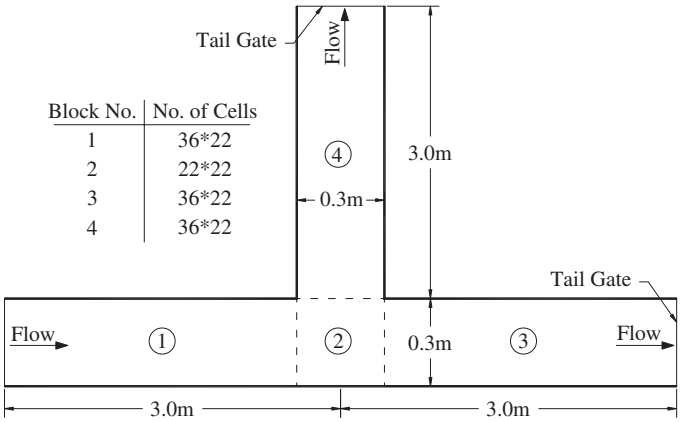

Figure 8 Block topology and number of grids in each block for side intake test case

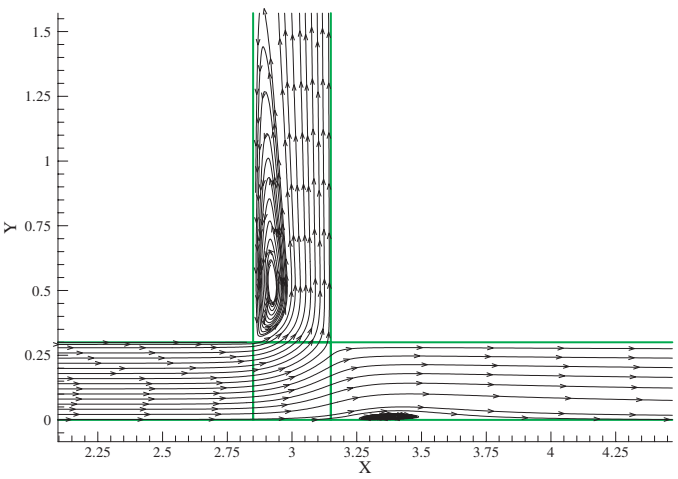

Figure 9 Flow pattern at side intake test case

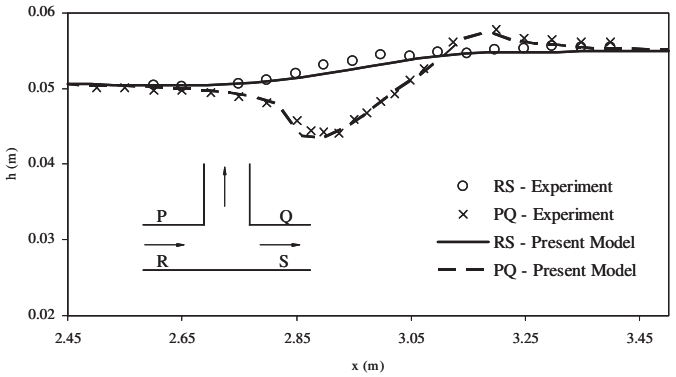

Figure 10 Flow depth along the main channel

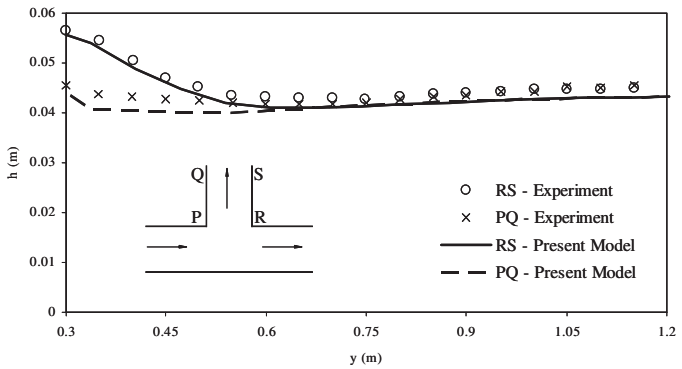

Figure 11 Flow depth along the intake channel

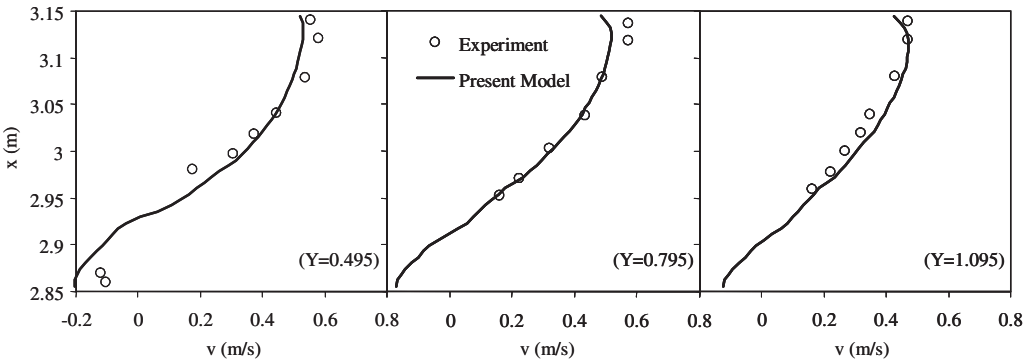

Figure 12 Depth averaged flow velocity along the intake channel

directions which implies finer mesh near walls and in the region near the junction. The flow pattern resulted by the model is shown in Fig. 9. This figure shows a large circulation zone in the side channel and a smaller circulation in the main channel which conforms to the experimental observation of Shettar and Murthy (1996). Water depth along 2 walls of main channel and side channel are compared with experimental data in Figs. 10 and 11. Also, the velocities along side and main channel are presented in Figs. 12 and 13 which are in good agreement with experimental data.

To show the efficiency of using under-relaxation factors, in this test case the model was executed disregarding the under-relaxation factors by setting them to unity. To get convergence a time step of $\Delta t = 0.1$ S was necessary and it took almost 1 min CPU time for getting convergence. With under-relaxation factors equal to 0.5, the time step could be increases to $\Delta t = 3$ S and after 7 S of CPU time convergence was achieved with the same initial condition.

The last test case is a jet forced laminar flow to a circular basin. This case is described in details elsewhere (Hadian and Zarrati, 2005). Totally 13 blocks were used to cover the flow domain as is presented in Fig. 14. Flow pattern calculated by the model is shown in Fig. 15 and velocity profile across the basin diameter is compared with other numerical models in Fig. 16. This figure shows satisfactory agreements between present model and other numerical models.

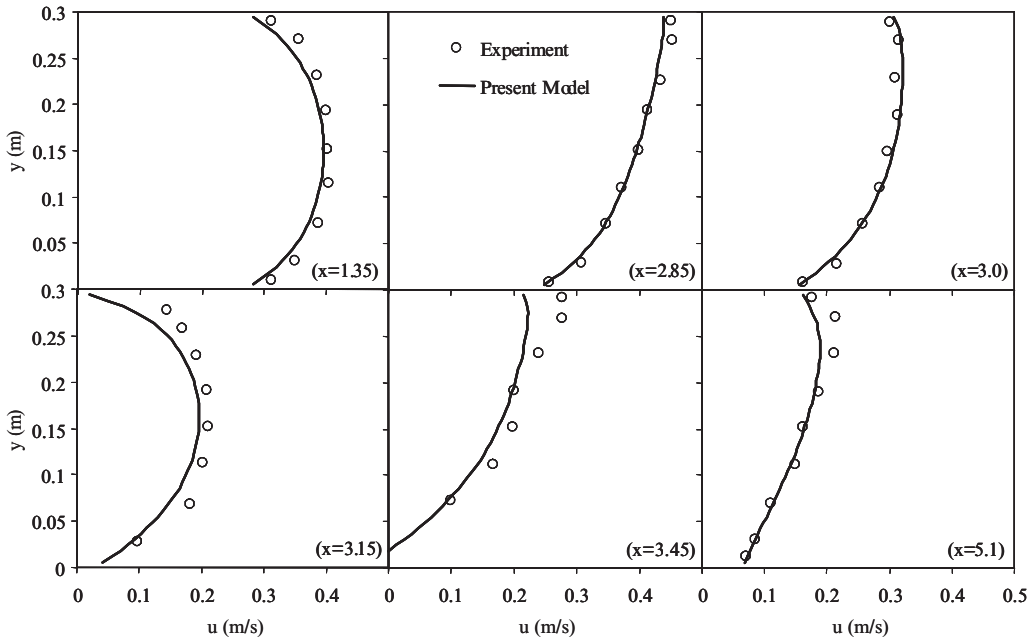

Figure 13 Depth averaged flow velocity along the main channel

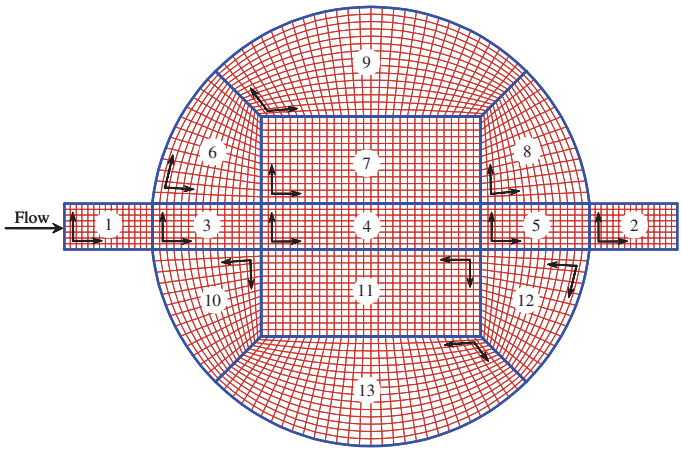

Figure 14 Selected block topology and generated mesh for the numerical model

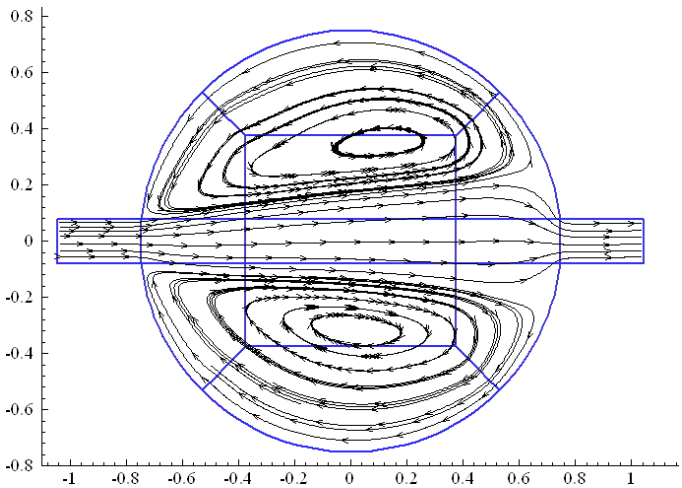

Figure 15 Predicted flow pattern in the circular basin by present model

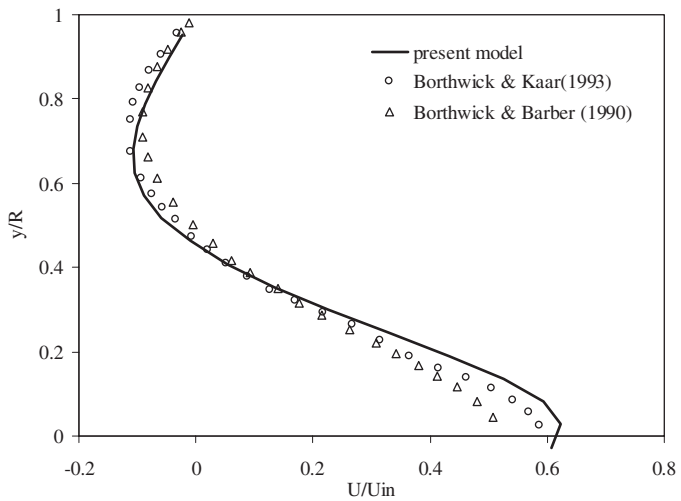

Figure 16 u-velocity profile along vertical diameter (half of the basin is presented)

6 Conclusion

Dealing with complex geometries is an important issue in solving the fluid flow problems. Different methods based on structured or unstructured grids have been developed for this purpose; each has its own merits and drawbacks. In the present study, to deal with complex flow domain with a more general method the Multi-Block technique was developed for solving 2-D free surface shallow flows. The governing equations were solved on a collocated grid arrangement by means of implicit method. To prevent checker board water surface oscillation, the momentum interpolation method was applied for cell face velocities. A SIMLEC-like algorithm was used for coupling water surface elevation and velocities. The model was verified by applying it to predict water surface profile in a straight channel with different block topologies, water surface and velocity profiles in the region near a side intake and velocity profile and flow pattern in

a laminar jet forced flow to a circular basin. The results of the model showed its applicability and robustness for simulating free surface flow problems with complex boundaries. The scheme presented here, is therefore a powerful tool for problems with complex flow domains such as flow in river confluences and bifurcations, flow around obstacles and river constriction. The method developed in this paper is extendable to 3-D models too.

Notation

A = Coefficients of discretized equations
D = Diffusive flux
F = Convective flux
U, V = Depth averaged contravariant velocities
J = Jacobian of transformation
Z_b = Bed elevation
g = Gravitational acceleration
h = Water depth
q_{ij} = Metric tensor
n = Manning's coefficient
t = Time
u, v = Depth averaged Cartesian velocities
u_* = Bed shear velocity
x, y = Cartesian coordinates
$x_\xi, x_\eta, y_\xi, y_\eta$ = Metrics
Γ = Diffusion coefficient
α = Under-relaxation factor
ϕ = u or v

Greek Symbols

κ = Von Karman constant (0.4).
ν = Kinematic viscosity of fluid
ν_e = Depth averaged effective viscosity
ν_t = Depth averaged turbulent viscosity
ρ = Water density
ξ, η = General curvilinear coordinates
τ_{bx}, τ_{by} = Bed shear stresses in x and y directions
ζ = Water surface elevation

Superscripts

** = Value of quantity from previous iteration
* = Value of quantity calculated by momentum equations' = quantity correction

Subscripts

P, E, W, N, S = Grid point and four neighboring points around it
nb = Neighboring points

References

Apsley, D., Hu, W. (2003). CFD simulation of two- and three-dimensional free surface flow. *Int. J. Numer. Methods Fluids* 42, 465–491.

Borthwick, A.G.L., Barber, R.W. (1990). prediction of low Reynolds number jet-forced flow inside a circle a using the Navier–Stokes equations. *Int. J. Numer. Methods Fluids* 4(3), 323–343.

Borthwich, A.G.L., Kaar, E.T. (1993). shallow flow modelling using curvilinear depth-averaged stream function and vorticity transport equations. *Int. J. Numer. Methods Fluids* 17, 417–445.

Chapman, R.S., Kuo, C.Y. (1985). Application of the two-equation k-ε turbulence model to a two-dimensional, steady, free surface flow problem with separation. *Int. J. Numer. Methods Fluids* 5, 257–268.

Choi, S.K. (1999). Note on the use of momentum interpolation method for unsteady flows. *Numerical Heat Transfer,* Part A 36, 545–550.

Chow, V.T. (1959). *Open Channel Hydraulics*. McGraw Hill Book Company.

Ferziger, J.H., Peric, M. (1996). *Computational Methods for Fluid Dynamics*. Corrected 2nd printing, Springer.

Hadian, M.R., Zarrati, A.R. (2005). Simulation of shallow flows in a circular basin using collocated multi-block method. *Proceeding of XXXI IAHR Congress*, Seoul, Korea.

Henshaw, W.D. (1994). A fourht-order accurate method for the incompressible Navier-Stokes equation on overlapping grid. *J. Comput. Phys.* 113, 13–25.

Hinatsu, M., Ferziger, J.H. (1991). Numerical computation of unsteady incompressible flow in complex geometry using a composite multigrid technique. *Int. J. Numer. Methods Fluids* 13, 971–997.

Jia, Y., Wang, S.S.Y. (1999). Numerical model for channel flow and morphological change studies. *J. Hydraul. Engng. ASCE* 125(9), 924–933.

Klonidis, A.J., Soulis, J.V. (2001). An Implicit Scheme for steady two-dimensional free-surface flow calculation. *J. Hydraul. Res. IAHR* 39(4), 393–402.

Kuipers, J., Vreugdenhil, C.B. (1973). Calculation of two-dimensional horizontal flow. *Rep. S163, Part 1*, Delft Hydraulics Lab., Delft, Netherlands.

Launder, B.E., Spalding, D.B. (1974). The numerical computation of turbulent flows. *Comput. Methods Appl. Mech. Eng.* 3, 269–289.

Lien, F.S., Chen, W.L., Leschziner, M.A. (1996). A multiblock implementation of non-orthogonal collocated finite volume algorithm for complex turbulent flows. *Int. J. Numer. Methods Fluids* 23, 567–588.

Lien, F.S., Leschziner, M.A. (1994a). Upstream monotonic interpolation for scalar transport with application to complex turbulent flows. *Int. J. Numer. Methods Fluids* 19, 527–548.

Lien, F.S., Leschziner, M.A. (1994b). A general non-orthogonal collocated finite volume algorithm for turbulent flow at all speeds incorporating second-moment turbulence-transport closure, Part 1: computational implementation. *Comput. Methods Appl. Mech. Eng.* 114, 123–148.

Majumdar, S. (1988). Role of underrelaxation in momentum interpolation for calculation of flow with nonstaggered grids. *Numer. Heat Transfer* 13, 125–132.

McGuirk, J.J., Rodi, W. (1978). A depth-averaged mathematical model for the near field of side discharge into open-channel flow. *J. Fluid Mech.* 86(4), 761–781.

Meakin, R.L., Street, R.L. (1988). Simulation of environmental flow problems in geometrically complex domain, Part 2: a domain-splitting method. *Comput. Methods Appl. Mech. Eng.* 68, 311–331.

Miller, T.F., Schmidt, F.W. (1988). Use of pressure-weighted interpolation method for the solution of the incopressible Navier-Stokes equations on a nonstaggered grid system. *Numerical Heat Transfer* 14, 213–233.

Molls, T., Chaudhry, M.H. (1995). Depth-averaged open-channel flow model. *J. Hydraul. Engng, ASCE* 121(6), 453–465.

Olsen, Nils Reidar, B. (2000). CFD algorithms for hydraulic engineering. Available at http://www.bygg.ntnu.no/∼nilsol/cfd/cfdalgo.pdf

Patankar, S.V. (1980). *Numer. Heat Transfer and Fluid Flow*, McGraw-Hill.

Peric, M. (1990). Analysis of pressure-velocity coupling on nonorthogonal grids. *Numer. Heat Transfer,* Part B 17, 63–82.

Rhie, C.M., Chow, W.L. (1983). Numerical study of the turbulent flow past an airfoil trailing edge separation. *AIAA Journal* 21(11), 1525–1532.

Shettar, A.S., Murthy, K.K. (1996). A numerical study of division of flow in open channels. *J. Hydraul. Res. IAHR* 34(5), 651–675.

Shyy, W., Liu, J., Wright, J. (1994). Pressure-based viscous flow computation using multiblock overlapped curvilinear grids. *Numer. Heat Transfer,* Part B 35, 39–59.

Shyy, W., Thakur, S.S., Ouyang, H., Liu, J., Blosch, E. (1997). *Computational Techniques for Complex Transport Phenomena*, Cambridge University Press.

Sinha, S.K., Sotiropoulos, F., Odgaard, J. (1998). Three-dimensional numerical model for flow through natural rivers. *J. Hydraul. Engng. ASCE* 124(1), 13–24.

Tingsanchali, T., Maheswaran, S. (1990). 2-D depth-averaged computation near groyne. *J. Hydraul. Engng. ASCE* 116(1), 71–86.

Tu, J.Y., Fuch, L. (1992). Overlapping grids and multigrid methods for three-dimensional unsteady flow calculations in IC engines". *Int. J. Numer. Methods Fluids* 15, 693–714.

Vregdenhill, C.B., Wijbenga, J.H.A. (1982). Computation of flow pattern in rivers. *J. Hydraul Div. ASCE* 108(HY11), 1296–1310.

Wang, Y., Komori, S. (1999). Comparison of using cartesian and covariant velocity components on non-orthogonal collocated grids. *Int. J. Numer. Methods Fluids* 31, 1265–1280.

Weerakoon, S.B., Tamai, N., Kavahara, Y. (2003). Depth-averaged flow computation at a river confluence. *Proceeding Ins. Civil Engrg. Water & Maritime Engrg.* 156(1), 73–83.

Wijbenga, J.H.A. (1985). Determination of flow patterns in rivers with curvilinear coordinates. *Proceeding 21st IAHR Congress*, Melbourne, Australia, 132–139.

Wright, J.A., Shyy, W. (1993). A pressure_based composite grid method for the Navier-Stokes equations. *J. Comput. Phys.* 107, 225–238.

Ye, J., McCorquodale, J.A. (1997). Depth-averaged hydrodynamic model in curvilinear collocated grid. *J. Hydraul. Engng. ASCE* 123(5), 380–388.

Yu, B., Kawaguchi, Y., Tao, W.Q., Ozoe, H. (2002a), Checkerboard pressure predictions due to the underrelaxation factor and time step size for a nonstaggered grid with momentum interpolation method. *Numerical Heat Transfer,* Part B 41, 85–94.

Yu, B., Tao, W.Q., Wei, J.J., Kawaguchi, Y., Toshio, T., Ozoe, H. (2002b), Discussion on momentum interpolation method for collocated grids of incompressible flow. *Numerical Heat Transfer,* Part B 42, 141–166.

Zarrati, A.R., Tamai, N., Jin, Y.C. (2005). Mathematical modeling of meandering channels with a generalized depth averaged model. *J. Hydraul. Engng. ASCE* 131(6), 467–475.

Zhang, Y., Jia, J., Wang, S.Y. (2004). A multi-block algorithm for two-dimensional hydrodynamic model. *Proceeding 6th International Conference on Hydro-Science and Engineering*, Brisbane, Australia.

Zhou, J.G. (1995). Velocity-depth coupling in shallow-water flows. *J. Hydraul. Engng. ASCE* 121(10), 717–724.